Ocean Systems Engineering, *Vol. 3, No. 3 (2013) 203-217*
DOI: http://dx.doi.org/10.12989/ose.2013.3.3.203

Enhancement of wave-energy-conversion efficiency of a single power buoy with inner dynamic system by intentional mismatching strategy

I.H. Cho*[1] and M.H. Kim[2]

[1]*Department of Ocean System Engineering, Jeju National University, Jeju 690-756, Korea*
[2]*Department of Civil Engineering, Texas A&M University, College Station, Texas, 77843, USA*

(Received August 12, 2013, Revised September 2, 2013, Accepted September 15, 2013)

Abstract. A PTO (power-take-off) mechanism by using relative heave motions between a floating buoy and its inner mass (magnet or amateur) is suggested. The inner power take-off system is characterized by a mass with linear stiffness and damping. A vertical truncated cylinder is selected as a buoy and a special station-keeping system is proposed to minimize pitch motions while not affecting heave motions. By numerical examples, it is seen that the maximum power can actually be obtained at the optimal spring and damper condition, as predicted by the developed WEC(wave energy converter) theory. Then, based on the developed theory, several design strategies are proposed to further enhance the maximum PTO, which includes the intentional mismatching among heave natural frequency of the buoy, natural frequency of the inner dynamic system, and peak frequency of input wave spectrum. By using the intentional mismatching strategy, the generated power is actually increased and the required damping value is significantly reduced, which is a big advantage in designing the proposed WEC with practical inner LEG (linear electric generator) system.

Keywords: WEC(wave energy converter); relative heave motion; inner dynamic system; LEG(linear electric generator); double resonance; maximum PTO(power take off); intentional mismatching; high performance band-width

1. Introduction

Ocean waves hold enormous energy. For instance, the harvestable wave power is estimated to be as much as 10 TW. However, ocean wave energy is highly underutilized until recently. The primary limiting factors are the efficiency of PTO(power take off) system, survivability in harsh storm conditions, and high installation/maintenance cost. During the past decades, numerous ideas have been proposed for harvesting wave energy (e.g., Evans 1976, Kim and Choi 1983, Gato and Falcão 1988, McCormick 2007, Grilli *et al*. 2007, Elwood *et al*. 2007, Koo and Kim 2010, Cho *et al*. 2012, Koo *et al*. 2012, Park *et al*. 2012). This paper proposes a new point absorber and its design strategy that enhances the effectiveness of PTO in dry condition (Cho *et al*. 2012) by taking

*Corresponding author, Professor, E-mail: m-kim3@neo.tamu.edu

http://www.techno-press.org/?journal=ose&subpage=7 ISSN: 2093-6702 (Print), 2093-677X (Online)

advantage of properly tuned relative heave motions between floating buoy and inner dynamic system.

The conceptual design of the WEC(wave energy converter) under consideration is shown at Fig. 1. It consists of a vertical-cylinder buoy and a submerged exterior torus frame with 3 legs for positioning, minimizing pitch motion, and extra power take-off when necessary. The legs are connected to the seabed through vertical tendons (vertical mooring). The top tensions of the tendons are provided by the net buoyancy of the torus-subbuoy-with-3-legs. For this purpose, light tendon materials, such as polyester, (Tahar and Kim 2008) are to be used. When the buoy contacts the frame, the possible friction in heave direction is avoided by using suitable rollers imbedded in the frame. In this regard, the heave motion of the buoy is independent and not influenced by the subbuoy-leg mooring system. The buoy pitch motions are also restrained by the presence of the submerged frame. Since the vertical motion of the subbuoy-leg system is restricted by tendons (Yang and Kim 2010, 2011), the relative motion between the subbuoy and cylindrical buoy is also large, which can be utilized for extra power generation through a wet LEG(linear electric generator) when necessary. Inside the buoy, there exists a dry LEG by utilizing the relative heave motion between the buoy and magnet mass connected to the buoy through spring and damper. This way, electricity can be generated from both inside and outside of the cylindrical buoy to maximize its efficiency. The simulation of the entire system including mooring liner can be done by a coupled time-domain program (e.g., Arcandra and Kim 2003, Kang *et al*. 2013). In the present study, however, it is assumed that the subbuoy-leg system is used only for station-keeping and minimizing pitch motions. Since there are no mooring lines directly connected to the cylindrical buoy, it can easily escape the worst storm after sinking the subbuoy to the seafloor by water ballast. Then, the buoy can be towed to a safe place. After storm, the reverse steps can be applied to restore to the original set up.

In the present paper, we focus only on the PTO by a LEG inside the buoy. It is driven by the relative heave motions between the buoy and inner dynamic unit. It is also assumed that the submerged frame is deeply submerged and slender enough not to appreciably influence the diffraction-radiation wave field around the cylinder buoy. The theoretical results can be complemented by more practical mismatching strategies for maximum power harvesting for the given sea spectrum. In the next two sections, the theory for optimal hydrodynamic efficiency for the buoy and inner PTO unit and how to improve the PTO effectiveness by using intentional mismatching strategies are presented through a series of numerical examples.

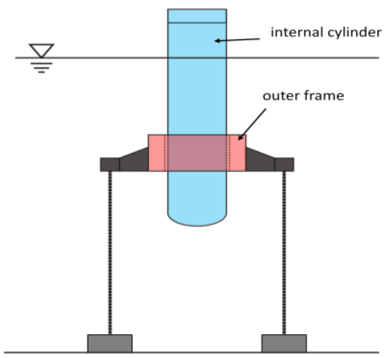

Fig. 1 Conceptual design of wave energy converter

2. Performance analysis

With this kind of arrangement, the pitch motion of the buoy, which may hamper the effectiveness of the heave-relative-motion-based PTO through coupling, can be reduced to minimal values. With the vertical mooring system, surge motions may be allowed but the surge mode is not coupled with the heave mode, so it does not affect the performance of the proposed power-generation system. The wave induced or surge-induced pitch motions can effectively be limited by the subbuoy-leg system with rollers. In this regard, the initial analysis for the performance of the proposed system is done by only considering the heave relative motions. The general strategy to achieve high performance is suggested through numerical examples. The present theory and methodology can straightforwardly be extended to arrays of such point absorbers, which will be the subject of forthcoming study.

Power-take-off through inner dynamic system inside a floating buoy is explained in Fig. 2. For simplification, the power take-off system is characterized by mass, linear stiffness, and linear damping. The inner system generates power through the relative heave motion between the buoy and inner mass (magnet or amateur). A systematic hydrodynamic theory dealing with the cylindrical buoy and the simplified inner PTO system (either hydraulic or LEG) is given as follows.

The LEG is inside the buoy (mass m_1) and for power take-off. The motion of a spar buoy induces the motion of the LEG system. The LEG dynamics in turn affect the motion of a spar buoy. The applied spring stiffness is k, damping c, and magnet mass m_2. We consider the two-body system as represented in Fig. 2. Let z and y be the heave motion of buoy and magnet. The equations of motion for the two-body system can be written by (Cho *et al*. 2012)

$$\begin{aligned} &(m_1+\mu)\ddot{z}+m_2\ddot{y}+B\dot{z}+\rho g S\, z=F_D, \\ &m_2\ddot{y}+c(\dot{y}-\dot{z})+k(y-z)=0, \end{aligned} \tag{1}$$

where the stiffness and damping coefficients, k and c represent controllable parameters.

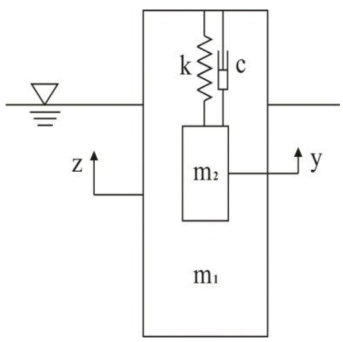

Fig. 2 Linear electric generator (LEG) by inner dynamic system

The mechanical power extracted from the relative velocity $\dot{x}(=\dot{y}-\dot{z})$ between the spar buoy and magnet is $P(t)=c\dot{x}^2$. The uncoupled and undamped natural frequency of the LEG system only is $\omega_G=\sqrt{k/m_2}$. The whole system is linear, we may write $z=z_o e^{-i\omega t}, y=y_o e^{-i\omega t}, x=x_o e^{-i\omega t}$ under the assumption of monochromatic incident waves of amplitude *A* and frequency ω. From Eq. (1), we obtain

$$\begin{aligned} &\left[-\omega^2(M+\mu)-i\omega B+\rho g S\right]z_o-\omega^2 m_2 x_o=AX, \\ &-\omega^2 m_2 z_o+\left(-\omega^2 m_2-i\omega c+k\right)x_o=0, \end{aligned} \tag{2}$$

where $M(=m_1+m_2)$ is a total mass, *S* is buoy water-plane area, *X* is heave wave exciting force per unit amplitude, μ is buoy added mass, and $B(=b+\nu)$ is total linear damping of buoy. After dividing Eq. (2) by $m_2\omega^2$ and rearranging Eq. (2) can be reduced to

$$\begin{aligned} &(U-iV)z_o-x_o=AQ, \\ &-z_o+\left(S-iT\right)x_o=0, \end{aligned} \tag{3}$$

which can readily be solved to give the heave amplitude of a spar buoy and the relative heave amplitude between the magnet and buoy normalized by incident wave amplitude A.

$$\begin{aligned} &\frac{x_o}{A}=\frac{Q}{(U-iV)(S-iT)-1}, \\ &\frac{z_o}{A}=\frac{(S-iV)Q}{(U-iV)(S-iT)-1}, \end{aligned} \tag{4}$$

where

$$U=\frac{\rho g S-\omega^2(M+\mu)}{m_2\omega^2}, V=\frac{B}{m_2\omega}, Q=\frac{X}{m_2\omega^2}, S=\frac{k}{m_2\omega^2}-1, T=\frac{c}{m_2\omega}.$$

Then, the time-averaged power per unit wave amplitude is given by

$$\begin{aligned} \frac{\bar{P}}{A^2}&=\frac{1}{2}c\omega^2\left|\frac{x_o}{A}\right|^2 \\ &=\frac{1}{2}\frac{c\omega^2\left|Q^2\right|}{\left|(U-iV)(S-iT)-1\right|^2} \\ &=\frac{1}{2}\frac{m_2\omega^3 T|Q|^2}{(US-VT-1)^2+(VS+UT)^2} \end{aligned} \tag{5}$$

To maximize $\bar{P}/A^2$ with respect to the two control parameters *S* and *T* (or k and c), we differentiate Eq. (5) with respect to *S* and *T*. Then, we obtain the conditions $S_{opt}=U/W^2, T_{opt}=V/W^2$ with $W^2=U^2+V^2$ for optimal power capture. Then, the maximum power take-off condition can be rewritten as

$$S_{opt} = \frac{k - m_2\omega^2}{m_2\omega^2} = \frac{m_2\omega^2\left(\rho g S - (M+\mu)\omega^2\right)}{\left(\rho g S - (M+\mu)\omega^2\right)^2 + (B\omega)^2},$$
$$T_{opt} = \frac{c}{m_2\omega} = \frac{m_2 B\omega^3}{\left(\rho g S - (M+\mu)\omega^2\right)^2 + (B\omega)^2}. \qquad (6)$$

By using the above two equations, the optimal stiffness and damping of the inner dynamic system can be determined from the given floater particulars and incident wave frequency.

2.1 Case 1: Use of double resonance

It is natural to assume that we can have the maximum PTO efficiency when the buoy natural frequency coincides with the maximum PTO frequency.

If ω in (6) is at the buoy heave resonance $(\rho g S - (M+\mu)\omega^2) = 0$ (or S_{opt} =0), then $k_{opt} = m_2\omega^2$. Considering the natural frequency of the inner unit $\omega_G = \sqrt{k/m_2}$, under the given condition buoy resonance frequency coincides with ω_G i.e., $\omega_o = \omega_G$. Therefore, it is called double-resonance condition. Under the same resonance condition, $T_{opt} = \frac{c}{m_2\omega} = \frac{m_2 B\omega^3}{(B\omega)^2} = \frac{m_2\omega}{B}$.

Considering $B = 2\kappa(M+\mu)\omega$ with κ being the buoy heave damping ratio, we obtain $c_{opt}/m_2\omega \approx 0.5$ for a special case of $m_2/M = 0.02, \kappa = 0.02$. If both conditions are satisfied, the corresponding power take-off becomes maximum for the given set up.

In irregular waves, it is impossible to satisfy the optimal condition for all component waves simultaneously. Therefore, a good choice is satisfying the condition for the peak frequency of the incident wave spectrum. For irregular waves, the heave-motion spectrum, the relative-heave-motion spectrum, and the square root power spectrum are computed from

$$S_z(\omega) = \left|\frac{z_o}{A}(\omega)\right|^2 \cdot S_\varsigma(\omega),$$
$$S_x(\omega) = \left|\frac{x_o}{A}(\omega)\right|^2 \cdot S_\varsigma(\omega),$$
$$S_{\sqrt{P}}(\omega) = \frac{\bar{P}(\omega)}{A^2} \cdot S_\varsigma(\omega). \qquad (7)$$

As the incident wave spectrum $S_\varsigma(\omega)$ in this section, the TMA spectrum (Bouws *et al.* 1985) is used for giving the possibility of developing a finite water depth form

$$S_\varsigma(\omega) = S_J(\omega) \cdot F(\omega_*) \qquad (8)$$

where $S_J(\omega)$ is the JONSWAP spectrum suggested by Goda(1988) and $F(\omega_*)$ is finite-depth factor. The significant buoy-heave amplitude, significant relative-heave-motion amplitude, and significant amplitude of square root power in irregular waves can then be obtained from

$$z_{a1/3} = 2\sqrt{\int_0^\infty S_z(\omega)d\omega}, x_{a1/3} = 2\sqrt{\int_0^\infty S_x(\omega)d\omega}, \sqrt{P}_{1/3} = 2\sqrt{\int_0^\infty S_{\sqrt{P}}(\omega)d\omega}. \quad (9)$$

An example calculation for the harvestable power is given in Fig. 3 for various values of k and c including the optimally tuned case. All the calculations for hydrodynamic coefficients and wave forces/body responses were extensively checked (Cho *et al*. 2012) by using two independently developed computer programs (eigen-function expansion method and boundary element method).

At the theoretical peak frequency, the optimal case actually generates the highest power, as predicted by the developed WEC theory. However, it is not necessarily so for the neighboring frequencies in case of the left figure (varying c for fixed k). Actually, the lower-than-optimal-damping value produces wider bandwidth for quality PTO. Therefore, under this condition, more wave energy may be harvestable. Table 1 illustrates such a case. In this case, less-than-optimal damping produces more power due to the reason explained in the above i.e. slightly smaller peak amplitude but wider high-quality band-width.

Table 1 Significant heave amplitude and significant square root power amplitude $(\sqrt{P_{1/3}})$ under double-resonance optimal(first row) and less-optimal(second row) conditions (k_{opt}, c_{opt}) for JONSWAP spectrum of $H_{1/3} = 2.0\,m, \omega_P = 1.4$ rad/sec, $\gamma = 3.3, h = 30\,m, d = 4.7\,m, 2a = 1.0\,m,$ and $m_2 / M = 0.02$

ω_G / ω_o	(k_{opt}, c_{opt})	$z_{o1/3}$ (m)	$x_{o1/3}$ (m)	$\sqrt{P_{1/3}}(W^{1/2})$
1.0	(148.1,49.45)	2.52	5.21	50.99
	(148.1, 10.0)	1.93	12.69	55.80

Table 2 Significant heave amplitude and significant square root power amplitude $(\sqrt{P_{1/3}})$ under double-resonance condition for $H_{1/3} = 2.0m, \omega_p = 1.39$ rad/sec, $c / m_2\omega_o = 0.5$, $k / m_2\omega_o^2 = 1.0$

ω_o / ω_P natural/peak freq ratio	d (m) draft	$z_{o1/3}$ (m) buoy heave	$x_{o1/3}$ (m) relative heave	$\sqrt{P_{1/3}}(W^{1/2})$ sqrt power
0.9	6.27	1.58	3.03	21.27
1.0	5.00	2.45	4.62	33.24
1.1	4.19	2.68	4.78	35.12
1.2	3.52	2.30	3.81	28.59

The above example is for the case $\omega_o = \omega_G = \omega_p$. For the given sea spectrum, the buoy resonance frequency can be adjusted by changing its draft so that the ratio of buoy resonance frequency ω_o to spectral-peak frequency ω_p can be varied. Table 2 actually shows that the maximum PTO is possible when the peak frequency is slightly lower than the buoy's heave natural frequency ω_o i.e., ω_o / ω_p =1.1. It shows that the slightly mismatched condition between buoy's heave natural frequency and peak spectral frequency produces the best power output. This kind of calculation can be used to determine the optimal buoy draft for the given buoy radius and sea spectrum, which needs to be taken into consideration in the actual design of the WEC.

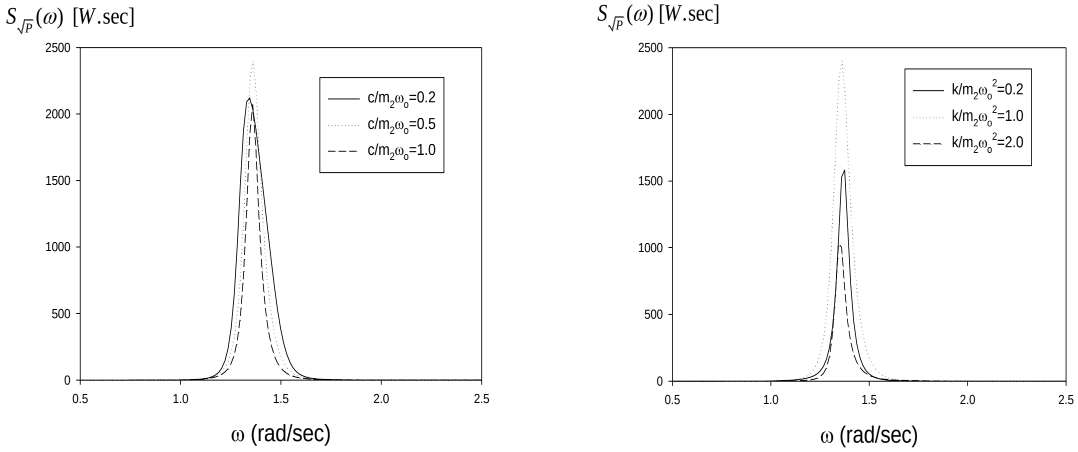

Fig. 3 Square root power spectrum as a function of wave frequency for various non-dimensional damping and stiffness for $H_{1/3} = 2.0m,\ \omega_P = 1.39\,\text{rad/sec}$, $(left) k / m_2\omega_o = 1.0$, $(right) c / m_2\omega_o = 0.5$

2.2 Case 2 Intentional mismatching of resonance frequencies between buoy and inner unit

In the previous section, we considered the case of double resonance ($\omega_o = \omega_G$). In this section, let us consider whether the PTO can even be enhanced by intentionally mismatching resonance frequencies between buoy and inner unit instead of double resonance. Since the optimal spring and damper condition (6) can be applied to any target frequency ω, we consider a special case of $\omega_{opt} = \omega_G \neq \omega_o$ and $\omega_o = \omega_p$. Then from (6)

$$\frac{k_{opt}}{m_2\omega_G^2} = 1 + \left(\frac{m_2}{M+\mu}\right)\frac{(\omega_G/\omega_o)^2\left(1-(\omega_G/\omega_o)^2\right)}{\left(1-(\omega_G/\omega_o)^2\right)^2 + 4\kappa^2(\omega_G/\omega_o)^2},$$
$$\frac{c_{opt}}{m_2\omega_G} = \left(\frac{2m_2}{M+\mu}\right)\frac{\kappa(\omega_G/\omega_o)^3}{\left(1-(\omega_G/\omega_o)^2\right)^2 + 4\kappa^2(\omega_G/\omega_o)^2}. \tag{10}$$

This equation can be used for further analysis of PTO effectiveness for the given non-double-resonance condition. After the buoy design is fixed, ω_G can easily be varied by modifying inner mass or inner spring. Fig. 4 shows the variation of optimal spring and damper for various inner-mass values for $\kappa = 0.02, \mu = 0.065M$, and $\omega_0 = \sqrt{\dfrac{\rho g S}{M + \mu}} = 1.4\,\text{rad/sec}$.

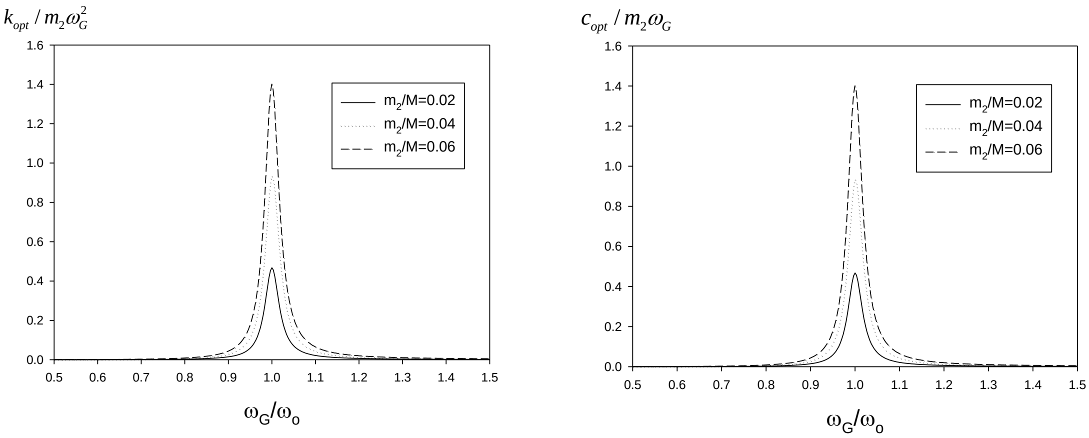

Fig. 4 Optimal parameters (k_{opt}, c_{opt}) for maximum power take-off as a function of the ratio of natural frequency between LEG and buoy system (ω_G / ω_o) for $\kappa = 0.02, \omega_o = 1.4\,\text{rad/sec}$

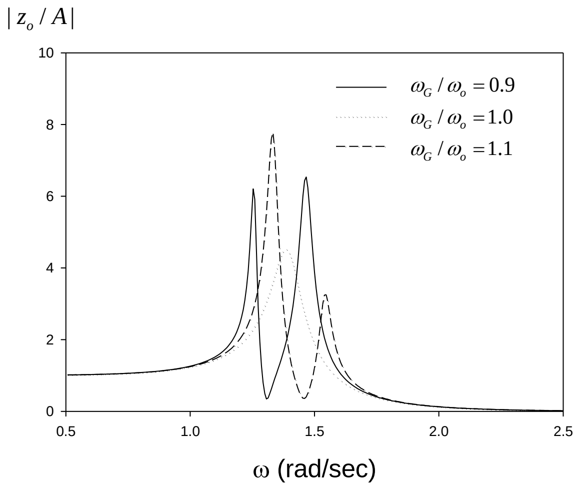

Fig. 5 Heave motion RAO of a spar buoy under optimal condition (k_{opt}, c_{opt}) as a function of resonant frequency ratio (ω_G / ω_o) and incident wave frequency for $m_2 / M = 0.02$

We can see that the magnitudes of optimal spring and damper increase as inner mass increases. Also, for any given inner mass, the required optimal stiffness and damping sharply increases at the double resonance condition. If ω_o and ω_G are slightly mismatched, the values of optimal stiffness and damping drop sharply, which is an attractive factor for the PTO designer.

From this point on, let us consider a particular case of $h = 30\,m, d = 4.7\,m, 2a = 1.0\,m$ and $m_2 / M = 0.02$. Figs. 5 and 6 plot the buoy heave RAO and buoy-inner-mass relative motion RAO as function of wave frequency in case the optimal k and c are applied. It can be seen that by slightly mismatching ω_o and ω_G, the buoy responses remain about the same but the relative motions can be greatly increased mainly due to the fact that the optimal damping values are small under the mismatched condition, which can also be viewed from Fig. 4. Since output power is proportional to PTO damping magnitude, the output power under the mismatched condition with smaller damping is not necessarily increased despite the large increase of relative motions, which can actually be seen in Fig. 7.

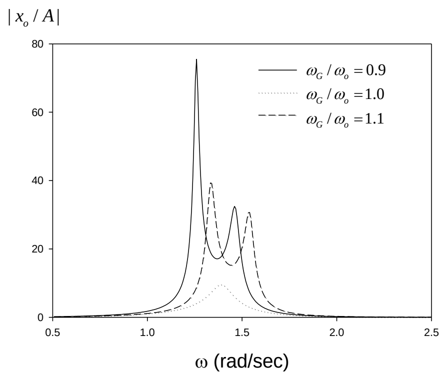

Fig. 6 Relative heave motion RAO of a magnet mass with respect to a spar buoy under optimal condition (k_{opt}, c_{opt}) as a function of resonant frequency ratio (ω_G / ω_o) and incident wave frequency for $m_2 / M = 0.02$

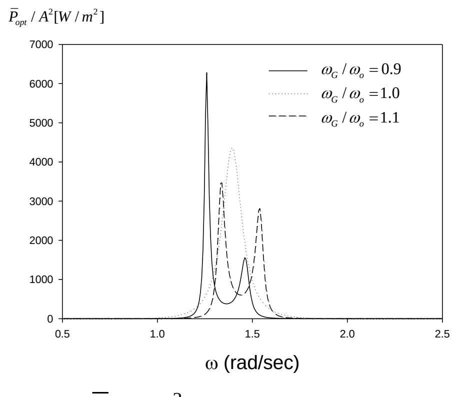

Fig. 7 Optimal time-averaged power($\bar{P}_{opt} / A^2$) as a function of resonant frequency ratio (ω_G / ω_o) and incident wave frequency for $m_2 / M = 0.02$

The actual power output for various mismatched conditions can be more clearly seen in a more realistic irregular sea. As the incident wave spectrum $S_\varsigma(\omega)$, the TMA spectrum (Bouws *et al.* 1985) is used for giving the possibility of developing a finite water depth form

$$S_\varsigma(\omega) = S_J(\omega) \cdot F(\omega_*) \quad (11)$$

where $S_J(\omega)$ is the JONSWAP spectrum with enhancement parameter $\gamma = 3.3$ and $F(\omega_*)$ is given by

$$F(\omega_*) = f^{-2}\left[1 + \frac{2\omega_* f}{\sinh(2\omega_* f)}\right]^{-1},$$

where $1 = f\tanh(\omega_*^2 f)$ and $\omega_*^2 = \dfrac{\omega^2 h}{g}$.

This wave amplitude spectrum is plotted in Fig. 8 as function of wave frequencies. In the same figure, the corresponding wave vertical-velocity spectrum is also given. Compared to wave amplitude spectrum, wave velocity spectrum has more useful energy in higher frequency region. Since power output is proportional to velocity squared, the high frequency region is generally very useful for WEC design. On the contrary, the low frequency swell, even if it has large energy, may not be so useful in view of velocity magnitude.

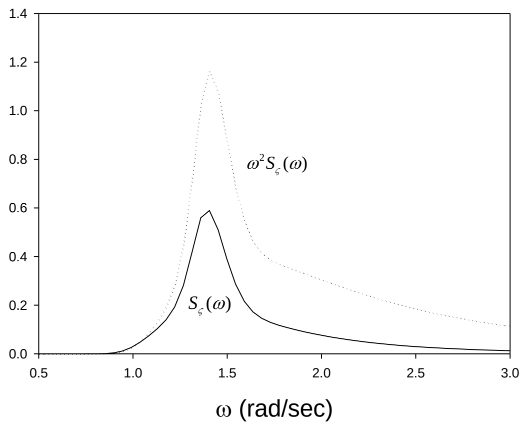

Fig. 8 JONSWAP Wave amplitude spectrum and the corresponding velocity spectrum for $H_{1/3} = 2.0\,m, \omega_P = 1.4$ rad/sec

The corresponding buoy-heave and buoy-inner-mass-relative-heave spectra are plotted in Figs. 9 and 10. It is seen that the relative heave motions are greatly increased as a result of intentional mismatching compared to the double-resonance case. However, as shown in Fig. 11, the actual increase of power is not obvious after mismatching. The corresponding results are tabulated in Table 3. As was pointed out in previous discussions, by intentional mismatching, about the same amount of power can be achieved with significantly smaller PTO damping, which is a very attractive factor to the WEC and PTO designers. However, if relative motions are too large, there may be wear-and-tear and fatigue issue for the inner dynamic system, so there should be some degree of compromise in the final selection of the optimal case. For instance, we actually have the best power output when ω_G / ω_o =1.05 with about six times smaller damping compared to the double-resonance case. The relative heave motions in this case are increased by 2.6 times compared to the double-resonance case.

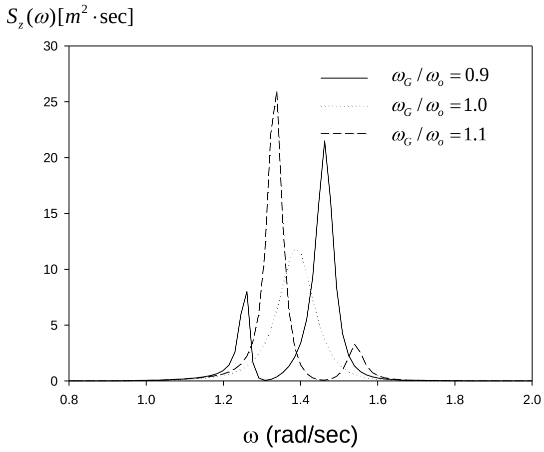

Fig. 9 Heave motion spectrum of a spar buoy under optimal condition (k_{opt}, c_{opt}) as a function of resonant frequency ratio (ω_G / ω_o) and incident wave frequency for $H_{1/3} = 2.0\, m, \omega_P = 1.4\, \text{rad/sec}$, $m_2 / M = 0.02$

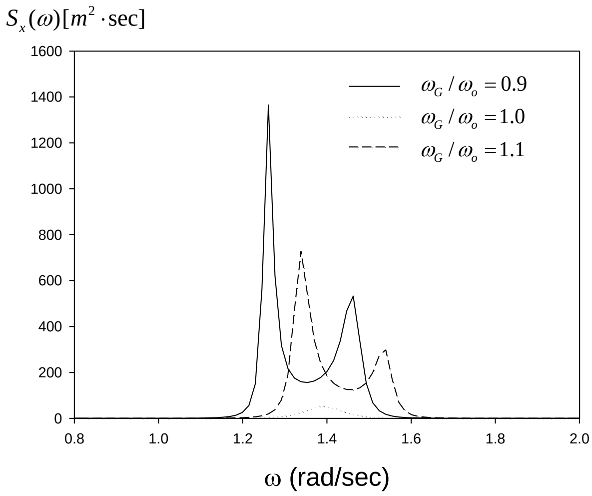

Fig. 10 Relative motion spectrum of a magnet mass with respect to a spar buoy under optimal condition (k_{opt}, c_{opt}) as a function of resonant frequency ratio (ω_G / ω_o) and incident wave frequency for $H_{1/3} = 2.0\, m, \omega_P = 1.4\, \text{rad/sec}$, $m_2 / M = 0.02$

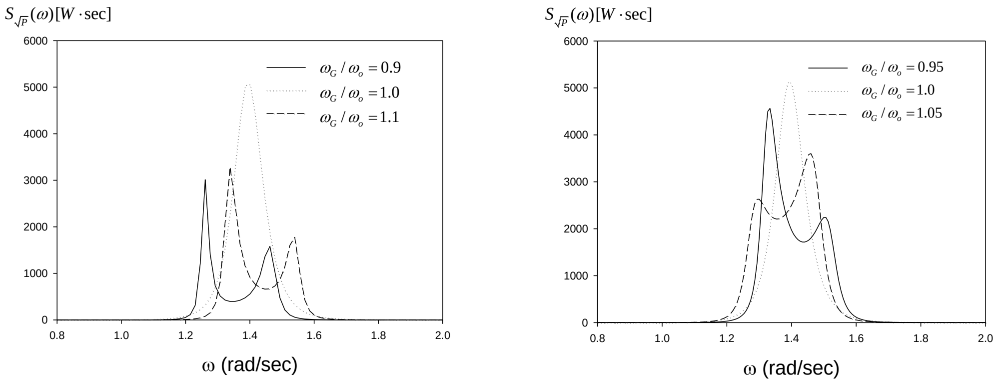

Fig. 11 Optimal square root power spectrum under optimal condition (k_{opt}, c_{opt}) as a function of resonant frequency ratio (ω_G/ω_o) and incident wave frequency for $H_{1/3}=2.0\,m, \omega_P=1.4\,\text{rad/sec}, m_2/M=0.02$

Table 3 Significant heave amplitude and significant square root power amplitude $(\sqrt{P}_{1/3})$ under optimal conditions (k_{opt}, c_{opt}) for $H_{1/3}=2.0\,m, \omega_P=1.4\,\text{rad/sec}, \ \gamma=3.3$

ω_G/ω_o	(k_{opt}, c_{opt})	$z_{o1/3}$ (m)	$x_{o1/3}$ (m)	$\sqrt{P_{1/3}}(W^{1/2})$
0.85	(112.1,0.53)	3.15	17.97	16.87
0.9	(129.2,1.39)	2.71	20.23	32.13
0.95	(153.7, 5.88)	2.17	15.05	50.96
1.0	(148.1,49.45)	2.52	5.21	50.99
1.05	(135.2, 7.84)	2.01	13.67	52.88
1.1	(160.7,2.52)	2.70	17.18	38.43
1.15	(181.2,1.30)	3.25	13.48	22.24

2.3 Case 3 Intentional mismatching of all three relevant frequencies

From the previous two sections, it is seen that the best choice is (i) when the buoy heave natural frequency is slightly above peak spectral frequency in case of double resonance $\omega_{opt}=\omega_G=\omega_o=\omega_p$, (ii) the natural frequency of inner system is slightly above buoy natural frequency in case $\omega_{opt}=\omega_G\neq\omega_o$ and $\omega_o=\omega_p$, and (iii) from Table 2, spectral peak frequency is slightly below the buoy natural frequency i.e., $\omega_{opt}=\omega_G\neq\omega_o>\omega_p$.

In this section, let us verify the third case, whose effectiveness is anticipated to be the best based on the previous discussions i.e. all three frequencies are slightly mismatched while optimal condition is targeted at ω_G.

Under this condition, to see the sensitivity against the location of the peak spectral frequency, the ratio of incident-wave spectral peak frequency and buoy-heave-resonance frequency ω_P/ω_o is varied from 0.5 to 1.5. Interestingly, we have the maximum power when its ratio is 0.9~0.95 instead of 1.0, whose trend is similar to that of Table 2. In Table 2, buoy draft is changed to vary the ratio ω_P / ω_o but in this case spectral peak is changed while draft remains constant. We also have the maximum power when ω_G / ω_o =1.05 i.e., it is better to locate the three relevant frequencies with 0.05rad/s interval. This can directly be seen from the actual calculation of this case i.e., $\omega_{opt} = \omega_G = 1.62$ rad/s , $\omega_o = 1.54$ rad/s , and $\omega_p = 1.4$ rad/s.

(k_{opt}, c_{opt})	$z_{o1/3}$ (m)	$x_{o1/3}$ (m)	$\sqrt{P_{1/3}}\,(W^{1/2})$
(133.2,6.97)	2.04	14.44	55.47

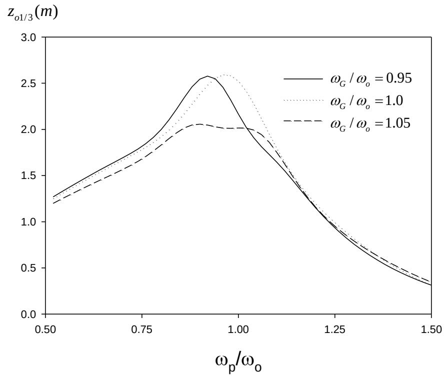

(a) Significant heave amplitude of buoy

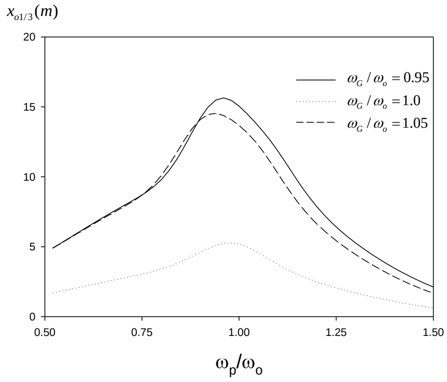

(b) Significant relative heave amplitude

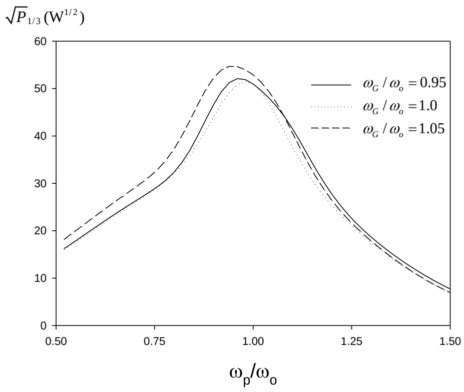

(c) Significant square root power amplitude

Fig. 12 Significant heave amplitude and significant square root power amplitude $(\sqrt{P_{1/3}})$ in irregular waves under optimal conditions (k_{opt}, c_{opt}) as a function of ω_G / ω_o and ω_P / ω_o for $H_{1/3} = 2.0\,m, m_2 / M = 0.02$

From Figs. 12(a) and (b), the mismatch of ω_o and ω_G greatly influences the increase of relative heave motions between the buoy and the inner mass regardless of spectral-peak locations, while the buoy heave responses remain about the same.

The fact that we had better locate buoy and inner-system resonance frequencies in the right side of input-wave spectral peak is related to that the incident-wave velocity spectrum, $\omega^2 S_{\varsigma}(\omega)$, has more skew toward higher frequencies, as can be seen in Fig. 8, and the power is proportional to wave velocity instead of wave amplitude. Fig. 12(c) and Table 3 are also relevant to possible active control of WEC with varying damping level depending on sea states. Such a variable damping level can be achieved by changing electro-magnetic field of WEC-LEG. The above factors need to be considered in the actual design of the WEC.

Under the given buoy and wave condition, when one selects the optimal frequency to be the peak of input wave spectrum, $\omega_{opt} = \omega_p$, with $\omega_p \neq \omega_G \neq \omega_o$, the resulting output power is smaller than the previous case. For example, when $\omega_{opt} = \omega_P = 1.4$ rad/s , $\omega_o = 1.54$ rad/s , and $\omega_G = \sqrt{\frac{k_{opt}}{m_2}} = 1.45$ rad/s, the output power is as follows

(k_{opt}, c_{opt})	$z_{o1/3}$ (m)	$x_{o1/3}$ (m)	$\sqrt{P}_{1/3}$ ($W^{1/2}$)
(133.2,1.525)	2.54	22.19	39.22

3. Conclusions

A LEG-based PTO (power-take-off) mechanism through a inner dynamic system of a floating buoy is suggested. For simplicity, the inner power take-off system is characterized by mass, stiffness, and damping and generates power through the relative heave motion between the buoy and inner mass. A systematic hydrodynamic theory is developed for the suggested WEC and the developed theory is illustrated by example calculations, which actually show that the maximum power can be obtained at the optimal condition of spring and damper, as predicted by the developed WEC theory. However, the band-width of high performance is not necessarily the greatest at the optimal (maximum-power-take-off) damping. Also, the maximum power can be obtained when heave-resonance frequency of the buoy is slightly higher than the peak of incident wave spectrum and the inner resonance frequency is slightly higher than the buoy heave resonance frequency, which needs to be taken into consideration in the actual design of the proposed WEC for irregular waves. Moreover, when the inner resonance frequency is slightly higher than the buoy heave resonance frequency, the required optimal damping value is significantly smaller than that of double-resonance condition, which is a big advantage in designing the inner LEG system. The undesirable pitch motions can effectively be restrained by the proposed station-keeping system without influencing the desired heave responses. More accurate time-domain numerical models including the actual buoy/mooring and LEG system (electro-magnetic forces) will be developed in the forthcoming study.

Acknowledgments

This work was supported by the New and Renewable Energy of the Korea Institute of Energy Technology Evaluation and Planning(KETEP) grant funded by the Korea government Ministry of Knowledge Economy.(2010302007 0080).

References

Arcandra and Kim, M.H. (2003), “Hull/mooring/riser coupled dynamic analysis and sensitivity study of a tanker-based FPSO”, *J. Appl. Ocean Res*., **25**(6), 367-382.

Bouws, F., Gunther, H., Rosenthal, W. and Vincent, C.L. (1985), “Similarity of the wind wave spectrum in finite depth water: 1. Spectral form”, *J. Geophys. Res*., **90**(1), 975-986.

Cho, I.H., Kim, M.H and Kweon, H.M. (2012), “Wave energy converter by using relative heave motion between buoy and inner dynamic system”, *Ocean Syst. Eng*., **2**(4), 297-314.

Elwood D., Rhinefrank K., Prudell J., Schacher A., Hogan P., Vander Meulen A., von Jouanne A., Brekken T., Yokochi A. and Yim S.C. (2007), “Experimental and numerical modeling of direct-drive wave energy extraction devices”, *Proceedings of the Offshore Mechanics and Arctic Engineering Conference*, San Diego, CA, Paper No.OMAE2007-29728.

Evans, D.V. (1976), “A theory for wave-power absorption by oscillating bodies”, *J. Fluid Mech*., **77**(1), 1-25.

Gato, L.M.C. and Falcão, A.F.de O. (1988), “Aerodynamics of the wells turbine”, *Int. J. Mech. Sci.*, **30**(6), 383-395.

Goda, Y. (1988), “Statistical variability of sea state parameters as a function of a wave spectrum”, *Coast. Eng. Japan*, **31**(1), 39-52.

Grilli, A.R., Merrill, J., Grilli, S.T., Spaulding, M.L. and Cheung, J. (2007), “Experimental and numerical study of spar buoy-magnet/spring oscillators used as wave energy absorbers”, *Proceedings of the 17th Intl. Conf. Offshore and Polar Eng*., No.2007-JSC-569.

Kang, H.S., Kim, M.H., Bhat, S.S. and Kang, H.Y. (2013), “Semi-active MR damper to reduce the dynamic response of top-tensioned riser”, *Proceedings of the Intl. Offshore Polar Engineering Conference*, ISOPE 2013, Anchorage

Kim, M.H. and Choi, H.S. (1983), “Hydrodynamic characteristics of two-dimensional wave energy absorbers”, *J. Soc. Naval Architect. Korea*, **20**(1).

Koo, W.C. and Kim, M.H. (2010), “A nonlinear time-domain simulation of a land-based oscillating water column (OWC) ”, *J. Waterway, Port C. Ocean - ASCE*, **136**(5), 276-285.

Koo, W.C., Kim, S.J. and Kim, M.H. (2012), “Numerical analysis of a floating wave energy converter BBDB(backward bent duct buoy) with different-shaped corners”, *Proceedings of the 30th Int. Offshore Mechanics and Arctic Eng. Conference*, Rio de Janeiro.

McCormick, M.E. (2007), *Ocean wave energy conversion*, Dover Publication.

Park, J.Y., Shin, S.H., Hong, K.Y. and Kim, S.H. (2012), “A study on the wave response and efficiency of a pendulum wave energy converter”, *Proceedings of the Intl. Offshore Polar Engineering Conference*, ISOPE 2012, Greece.

Tahar, A. and Kim, M.H. (2008), “Coupled dynamic analysis of floating structures with polyester mooring lines” , *Ocean Eng*., **35**(17-18), 1676-1685.

Yang, C.K. and Kim, M.H. (2010), “Transient effects of tendon disconnection of a TLP by hull-tendon-riser coupled dynamic analysis”, *Ocean Eng*., **37**(9), 678-687.

Yang, C.K. and Kim, M.H. (2011), “The structural safety assessment of a tie-down system on a TLP during hurricane events”, *Ocean Syst. Eng*., **1**(4), 263-283.